

Load-slip curves of shear connection in composite structures: prediction based on ANNs

Kai Guo^{1,2} and Guotao Yang*¹

¹School of Civil Engineering, Qingdao University of Technology, Qingdao 266033, China

²College of Architecture and Civil Engineering, Beijing University of Technology, Beijing 100124, China

(Received November 21, 2019, Revised July 30, 2020, Accepted July 31, 2020)

Abstract. The load-slip relationship of the shear connection is an important parameter in design and analysis of composite structures. In this paper, a load-slip curve prediction method of the shear connection based on the artificial neural networks (ANNs) is proposed. The factors which are significantly related to the structural and deformation performance of the connection are selected, and the shear stiffness of shear connections and the transverse coordinate slip value of the load-slip curve are taken as the input parameters of the network. Load values corresponding to the slip values are used as the output parameter. A two-layer hidden layer network with 15 nodes and 10 nodes is designed. The test data of two different forms of shear connections, the stud shear connection and the perforated shear connection with flange heads, are collected from the previous literatures, and the data of six specimens are selected as the two prediction data sets, while the data of other specimens are used to train the neural networks. Two trained networks are used to predict the load-slip curves of their corresponding prediction data sets, and the ratio method is used to study the proximity between the prediction loads and the test loads. Results show that the load-slip curves predicted by the networks agree well with the test curves.

Keywords: load-slip curve; artificial neural networks; shear stiffness; stud shear connection; perforated shear connection with flange heads

1. Introduction

Steel-concrete composite structures have been paid more and more attention by engineers and researchers for their excellent performance since they emerged from the beginning. Steel-concrete composite structures have been widely used in high-rise buildings, bridge structures, spatial structures and other engineering structures. As far as the bridge structures are concerned, composite structures are no longer only used in small span composite beam bridges, but also widely used in composite towers, cable tower anchorage areas, hybrid beams and other long-span bridge structures (Liu *et al.* 2003). Steel-concrete composite structures with the shear connections to combine concretes and steel components compensate the defects of insufficient ductility of the concrete and easy corrosion of the steel (Nie *et al.* 2005). The shear connection is an important component to ensure the steel and the concrete work together (Shahabi *et al.* 2016). In order to design composite structures scientifically and ensure the overall working performance, it is very important to obtain the shear performance of the shear connection. At present, the shear connections widely used in engineering are the stud shear connection and the perfobond rib shear connection (Gu *et al.* 2019).

As a type of flexible connection, the stud shear connection has isotropic shear performance and thus can guarantee the construction quality (Pavlovic *et al.* 2013). Composite structures will be out of shape under the shear load, so the nonlinear analysis needs to be conducted based on the load-slip constitutive relation of the stud shear connection on the combination surface. Hawkins proved that when the shear load value is low, the stud can be simulated as elastic flexible anchor bolt to predict its stress-slip curve under the shear force (Hawkins 1973). Johnson and May defined the stiffness of the stud shear connection as the slope of the secant line at half of its ultimate shear capacity (Johnson and May 1975). Lloyd and Wright proved that the stiffness data of stud shear connections are discrete, and it is difficult to regress them with an expression (Lloyd and Wright 1990). Oehlers and Johnson pointed out that there is a ductile platform for the load-slip curve of the stud shear connection and it is destroyed as a whole under the monotone load (Oehlers and Johnson 1987). Wang held that the shear stiffness of the stud shear connection can be conservatively determined as the secant stiffness at the design strength with an equivalent slip of 0.8 mm, and that the shear stiffness is uniformly distributed along the length (Wang 1998).

Belonging to rigid connections, the perfobond rib shear connection has a higher shear strength, a higher stiffness and the better fatigue resistance than the stud shear connection (Oguejiofor and Hosain 1994). The concrete splitting is a common failure mode of specimens containing perfobond rib shear connections under the shear load (He *et al.* 2016). Ahn *et al.* observed that the PBL shear connection

*Corresponding author, Professor
E-mail: yangguotao@qut.edu.cn

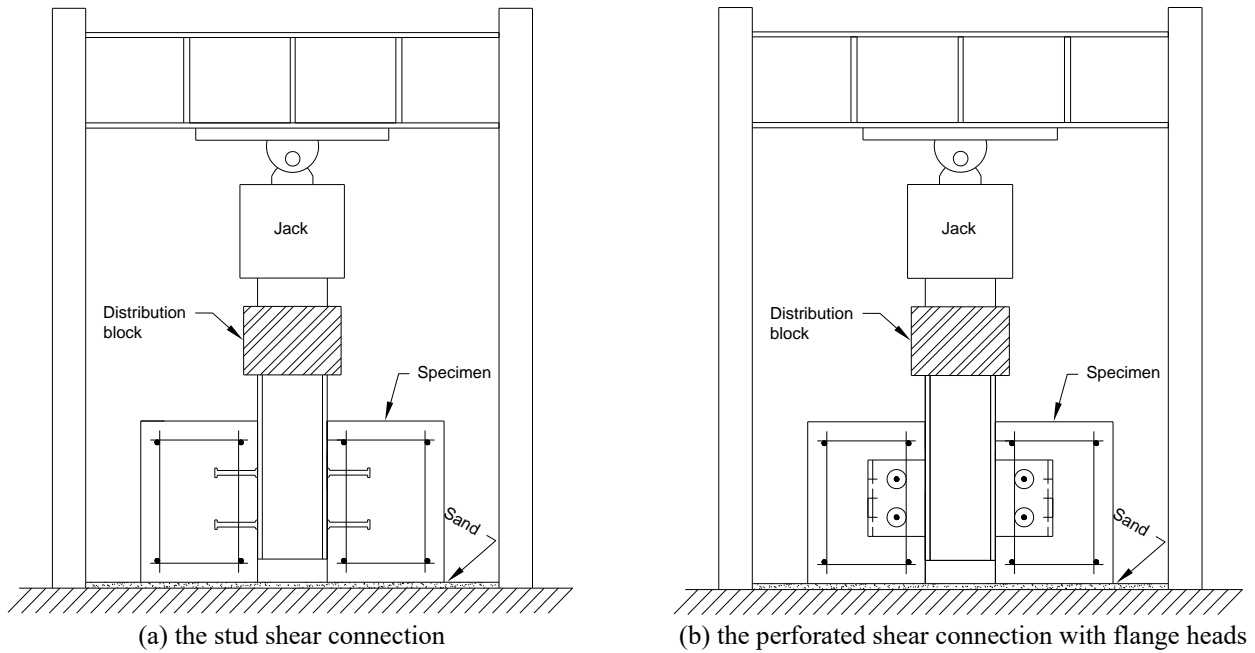


Fig. 1 The push-out test setup and layout

with end-bearing has the better shear capacity and ductility than that with no end-bearing (Ahn *et al.* 2008). Taking the beam on the elastic foundation as an example, Zheng derived the theoretical formula for calculating the initial shear stiffness of single-hole PBL shear connectors and proved its reliability through a push-out test (Zheng and Liu 2014). Vianna *et al.* developed the T-Perfobond shear connection to improve shear resistance, and quantified its shear properties through experiments (Vianna *et al.* 2008). The perforated shear connection with flange heads used in this paper not only maintains a high shear strength, but also has a good ductility (Su *et al.* 2014). Therefore, it is necessary to study the load-slip constitutive relation of the perforated shear connection with flange heads.

There are many factors that affect the shear connection performance of composite structures. So far, it is impossible to include all the factors in a unified formula. When the conditions change, different formulas need to be adopted for calculations, in which case the classification and discussion steps are tedious, and the workload is increased. Fortunately, there is no need to give specific mathematical expressions for the application of the neural network method, and as long as there are enough typical data sets for learning, the trained neural network can get the output results with the ideal accuracy through new input parameters (Zhao and Ren 2002). The neural network applied in this paper is the BP neural network which is improved by adding the error back propagation algorithm on the basis of the perceptron. Therefore, it has an effective weight adjustment algorithm to solve the classification problem of two kinds of linearly inseparable samples which cannot be processed by the perceptron (Rosenblatt 1958, Segal 1988). The load-slip curve of the shear connection of composite structures under the shear load is nonlinear, and the BP neural network can be trained according to

representative data sets to achieve the purpose of nonlinear mapping of parameters in training data sets and other similar data sets. Thus it is appropriate to use the BP neural network to predict the load-slip curve of shear connections.

2. Methodology

2.1 Push-out test

The effect of the shear connection of composite structures is to resist the relative slip and to transfer the shear force between concretes and steel beams (Bonilla *et al.* 2019). The test research has always been the main means of studying the performance of the shear connection which is in a force state close to the pure shear in the push-out test, so the results of push-out tests can reflect the bearing capacity of shear connections under the pure shear condition (Hallmark *et al.* 2019).

The push-out test setup is shown in Fig. 1. The vertical load is applied to the specimen through a hydraulic Jack in a self-balancing frame (Su *et al.* 2014). The Jack acts directly on a distributed beam, and then the load is transferred to the specimen by the distributed beam, which is to ensure the symmetrical force on both sides of the specimen. The specimen is composed of the steel beam, concrete blocks and shear connections welded on the steel beam and embedded in concrete blocks. The shear performance varies among different structures of shear connections (Wang *et al.* 2015). Generally, the shear connection is welded to the steel beam first, and then the concrete is formed in the corresponding position. In formed specimens, the steel beam has a distance from the ground as a whole, and the upper end is a part higher than the concrete block to meet the distance requirement for the pushed-out

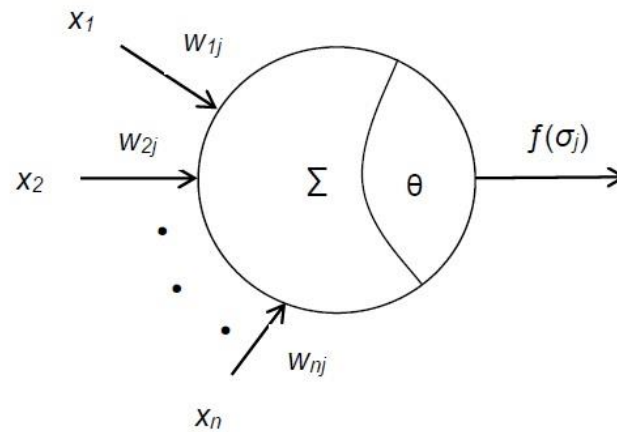


Fig. 2 The structure of an artificial neuron

steel beam. When there appears a load in the test, the steel beam is continuously pressed down, and a relative slip occurs between the steel beam and the concrete block, and the load increases until the specimen is destroyed (Chu *et al.* 2016).

Because of its accurate reflection of the shear performance of specimens, the push-out test is often used to study the influence of various factors on the performance of shear connections (Ning *et al.* 2019). Before the test begins, parameters to be considered should be determined. When the influences of different parameters on the stress and deformation performance of specimens are researched, specimens should be grouped to determine the unique variable parameter of each group (Ding *et al.* 2017).

Based on previous studies, some parameters which have a significant influence on the shear connection performance are selected from possible influencing factors, and the effects of other parameters on shear connection properties are ignored. Parameters of stud shear connections selected in this paper contain the concrete standard compressive strength (f_{ck}), the stud diameter (d_s), the stud ultimate tensile strength (f_{su}), the unilateral welding stud arrangement number (*Number*) and the concrete elastic modulus (E_c). The selected parameters of perforated shear connections with flange heads include the measured value of concrete compressive strength ($f_{c,m}$), the diameter of reinforcing bars (d_{pr}), the plate thickness (t_p), the hole diameter of web (d_h), the connection height (h_p) and the flange number (N_f).

2.2 Back propagation ANN

A BP artificial neural network generally contains nodes (i.e., neurons) with three attributes, namely, the input layer node, the hidden layer node and the output layer node (Mashhadban *et al.* 2016). Each node accepts the signal input of the previous node and outputs the signal after its own processing to the next node (Al-Shamiri *et al.* 2019).

The neuron model structure of the BP neural network is shown in Fig. 2. The neuron is the one in its layer, x_i is the output value of each neuron in the upper layer, w_{ij} is the weight that x_i passes to the neuron. They are multiplied and

accumulated, and the result is subtracted from the threshold θ , and the input value of the neuron (σ_j) is obtained. The neuron's excitation function [$f(\bullet)$] represents a kind of differentiable function, such as the sigmoid function, the linear function, etc., to get the output value of the neuron. The mathematical expression (Hammoudi *et al.* 2019) is as follows

$$f(\sigma_j) = f\left(\sum_{i=1}^n w_{ij}x_i - \theta\right) \quad (1)$$

The correction rule of the connection weight is as follows (Bui *et al.* 2018)

$$w_{ij}(k+1) = w_{ij}(k) + \eta \delta_j(k) x_i(k) \quad (2)$$

where k is the number of iterations, η is the step size of the weight correction, $\delta_j(k)$ is the partial derivative of the error energy function to σ_j .

2.3 Specific prediction model

In section 2.1 above, according to results of previous experiments, the key influencing factors of two kinds of shear connections are predicted, and an obvious relativity between shear connections and the ultimate shear capacity are proved. The ultimate shear capacity and its corresponding peak slip have significant influences on the shape of the load-slip curve of shear connections (He *et al.* 2017). Therefore, the key influencing factors selected above can be used as parameters to predict the load-slip curve of shear connections.

At the beginning of loading, the load-slip curve of shear connections is approximately linear, and the load value of shear connections increases rapidly with the increase of the slip value. However, when the slip reaches a certain critical position, the increase of load value slows down with the increase of the slip value (Nasrollahi *et al.* 2018). Considering the above changing process, this paper selects the 1 mm slip value as the dividing point when predicting the load-slip curve of shear connections. Select 0.1 mm slip

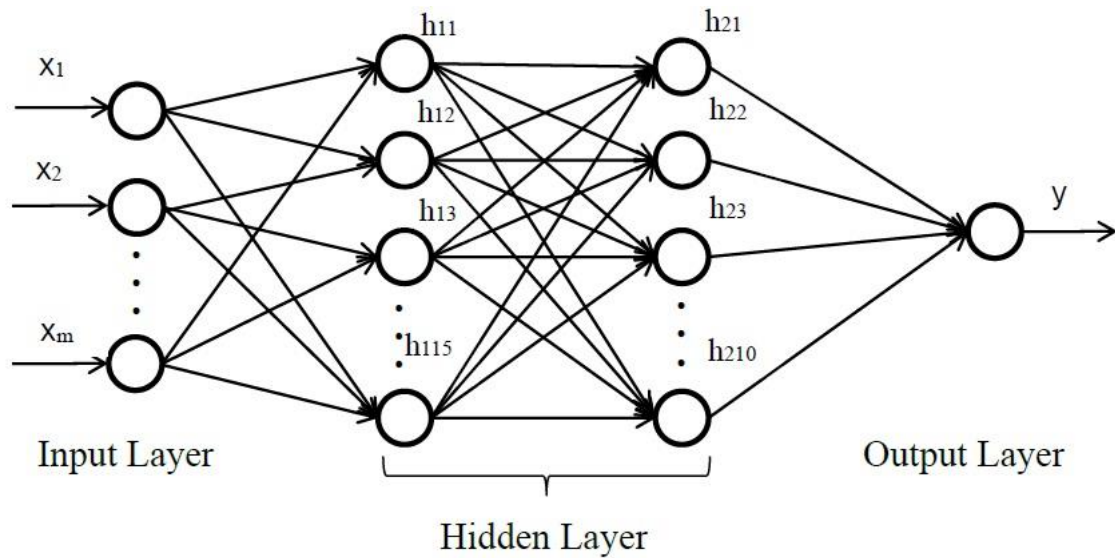


Fig. 3 The structure of an artificial neuron network for predicting the load-slip curves

value as the spacing in $[0, 1 \text{ mm}]$ interval, and when the slip value is larger than 1 mm, one data point is selected every 0.5 mm. Because of the phenomenon of zero drift and the problem of the instrument accuracy in the test, the load value is not always zero when the slip value is zero. In this case, the artificial specified slip value is zero for the unloaded state, and the corresponding load value is also zero.

In addition, the shear stiffness (K) also has a significant effect on the load-slip constitutive relation of shear connections. The European standard Eurocode 4 (EN 1994-1-1) defines this measure as $0.7 PRk / s$ in Clause A.3(3), where s is the slip at a load of $0.7 PRk$ and PRk is the characteristic resistance of the shear connector (Hicks and Smith 2014). In addition to the accepted code, many researchers have proposed different ways to define the shear stiffness (Nguyen and Machacek 2016, Suwaed and Karavasilis 2018, Wei *et al.* 2018, Kim *et al.* 2019). In this paper, the secant slope of the data point corresponding to the slip value of 0.2 mm on the load-slip curve is defined as the shear stiffness of the stud shear connection. When the slip value on the load-slip curve of the perforated shear connection with flange heads is 1 mm, the secant slope of the corresponding data point is the shear stiffness of the perforated shear connection with flange heads, for the test data are obtained from the images and the data points with slip values less than 1 mm are more likely to have errors.

After several attempts, the network structure of the input layer with m ($m = 7, 8$) nodes, the two-layer hidden layer with 15 nodes and 10 nodes, and the output layer with 1 node is determined. The topology of the network is shown in Fig. 3.

3. Application

3.1 Stud shear connection

Test data used in this section to train the BP neural network model and predict load-slip curves of stud shear connections are obtained from the reference (Wang 2013). A total of 21 groups of test data from deformations to failures under the shear force are obtained. The number of data bars in each group is not the same. Under the same data selection condition, the reason for this gap is that the ultimate bearing capacity and its corresponding peak slip of each stud shear connection are different.

On the whole, when conditions other than the shear stiffness are the same, there are 14 data groups among the 21 data groups that make up 7 pairs of pairwise comparisons, which shows that the greater the stiffness of the stud connection gets, the higher the shear strength becomes. Excluding one group that cannot be compared alone, the conclusion of comparisons of the remaining six groups is opposite, which may be due to the fact the stiffness defined in this paper cannot represent the stiffness characteristics of all connections. If the shear stiffness is defined more reasonably, the proportion of this part of data will decrease. Therefore, the shear stiffness of the stud shear connection is selected as a key factor among influencing factors.

Since each group of data is measured by the same stud shear connection after being loaded by the push-out test, the other key parameters are the same except for the shear force value and slip value. The key parameters data of 21 groups of stud shear connections are shown in Table 1.

The key parameters predicting load-slip curves of stud shear connections are as follows: the concrete standard compressive strength (f_{ck}), the stud diameter (d_s), the stud ultimate tensile strength (f_{su}), the unilateral welding stud arrangement number (*Number*), the concrete elastic modulus (E_c), the shear stiffness (K) and the slip value (*Slip*). For the stud length obtained from the reference is all 200 mm, it is not considered as a variable.

Table 1 Parameters of test specimens of stud shear connections

Specimen	d_s (mm)	f_{ck} (MPa)	E_c (GPa)	f_{su} (MPa)	Number	K (kN/mm)
SS-5-2	22	45.0	37.1	465.0	2	399.70
SS-6-1	22	45.0	37.1	675.0	2	545.12
SS-6-2	22	45.0	37.1	675.0	2	462.85
SS-7-1	25	45.0	37.1	485.0	2	394.41
SS-7-2	25	45.0	37.1	485.0	2	447.86
SS-8-1	30	45.0	37.1	430.0	2	701.11
SS-8-2	30	45.0	37.1	430.0	2	754.99
SS-19-1	22	33.5	34.6	515.0	2	372.86
SS-19-2	22	33.5	34.6	515.0	2	446.48
SS-20-1	22	33.5	34.6	515.0	4	319.78
SS-20-2	22	33.5	34.6	515.0	4	292.59
SS-21-1	22	33.5	34.6	515.0	6	243.43
SS-21-2	22	33.5	34.6	515.0	6	196.23
SS-22-1	22	33.5	34.6	515.0	9	315.97
SS-22-2	22	33.5	34.6	515.0	9	257.80
SS-24-1	25	37.0	35.5	515.0	4	438.52
SS-24-2	25	37.0	35.5	515.0	4	351.08
SS-25-1	25	37.0	35.5	515.0	6	372.31
SS-25-2	25	37.0	35.5	515.0	6	330.09
SS-26-1	25	37.0	35.5	515.0	9	374.86
SS-26-2	25	37.0	35.5	515.0	9	443.35

All the studs meet the requirement that the ratio of the stud length to the diameter is greater than 4, in which case the length of the stud has little effect on the deformation performance of the stud shear connection (Wang 2013). As a result, the mapping relationship can be expressed as

$$\text{Mapping} : P = \{d_s, f_{ck}, E_c, f_{su}, \text{Number}, K, \text{Slip}\} \rightarrow \text{Load} \quad (3)$$

where *Load* represents the load on the stud shear connection when the slip value is *Slip*.

40% of the training data are selected to test and validate the training network, so 18 in 21 groups of data are used for the network training, and the other 3 group of data for the prediction. As for the selection of predicting data, three groups of stud shear connections with different influencing factors are intentionally chosen in order to reflect learning results of the internal influence mechanism of the neural network on the change of the load value caused by the change of each key parameter. The stud shear connection numbers corresponding to three groups of data used for the prediction are SS-8-1, SS-20-2 and SS-26-1.

The training stops and the network passes through 26 iterations when the mean squared error of the network is 9.44. The stop state is shown in Fig. 4. It meets the requirement of the target error. In fact, when the error of the training set falls below 10, the validation set error curve doesn't drop again for six consecutive iterations, and the training terminates. Continuing to train the network may

overfit and the network performance is no longer improved (Lefik 2013), so the target error is set to 10.

The correlation degree curves between predicted data and experimental data are shown in Fig. 5. The predicted values in curves are positively correlated with the experimental values, and there is a relatively good consistency. The predictions of some zero data in the training correlation curve is not correct, and it is magnified in the test correlation curve. It might be because that the number of samples in the training data set is too small, and the calibration effect of zero points (the corresponding load value is 0 when the slip value is 0) is weaker than the influence of the overall data trend on the prediction. However, the zero point has been defined and stated that it is an unstressed state, the accuracy of the prediction data of it is of no practical significance on the stress and the deformation of shear connections. Therefore, it is unnecessary to pay attention to it in the comparative analysis of test results and prediction results.

Slip values in the input vector are selected from the zero to the peak slip value according to the rules when the specimens SS-8-1 and SS-20-2 are predicted. In order to compare with the other two curves, slip values of the specimen SS-26-1 are selected from the zero to 2 mm before the peak slip value. As can be seen from Fig. 6, the prediction curve coincides with the test curve in the rapid rise stage of the load-slip curve, but when the slip increases

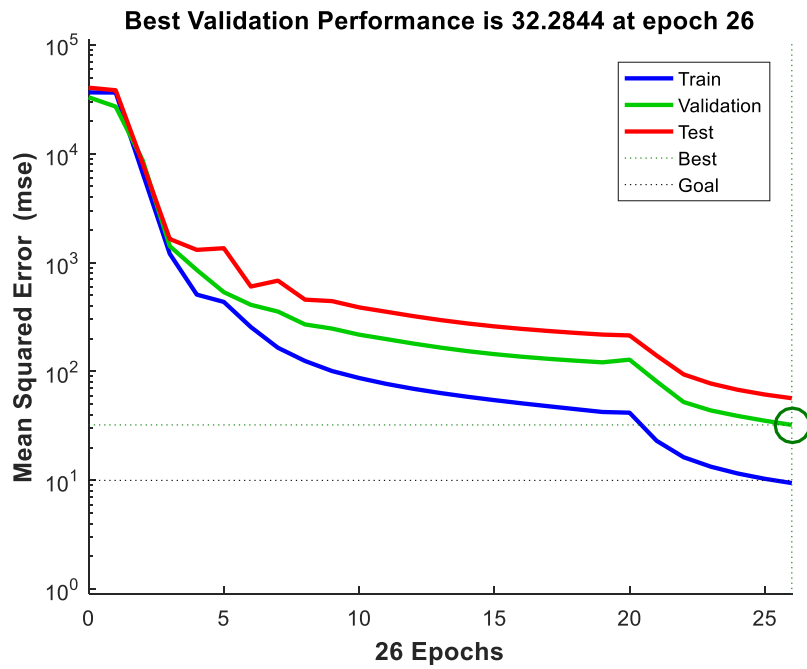


Fig. 4 Error declining curves of stud shear connections

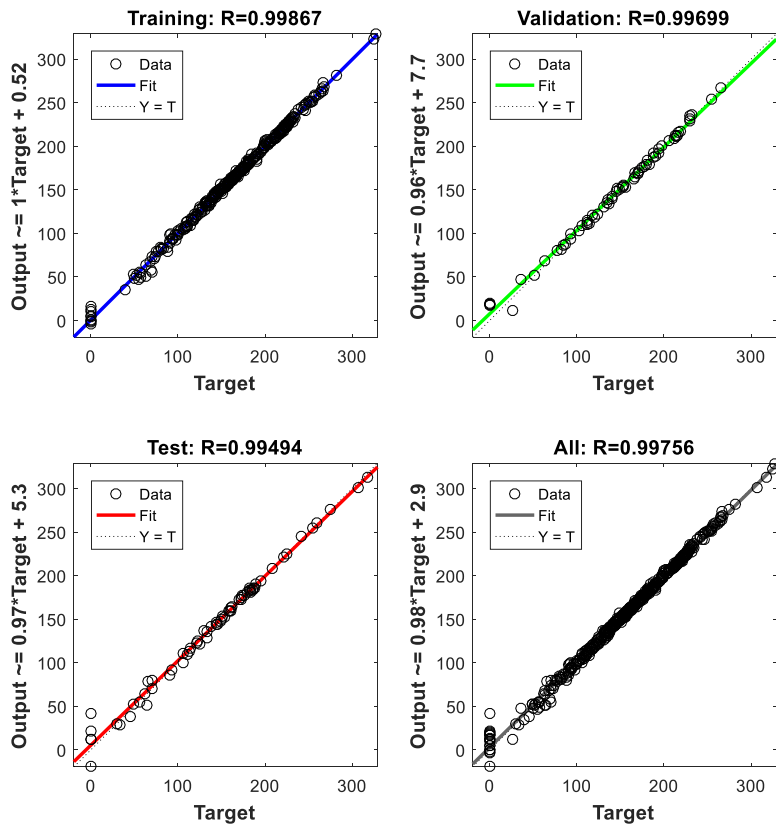


Fig. 5 The degree of correlations between tests and predictions of stud shear connections

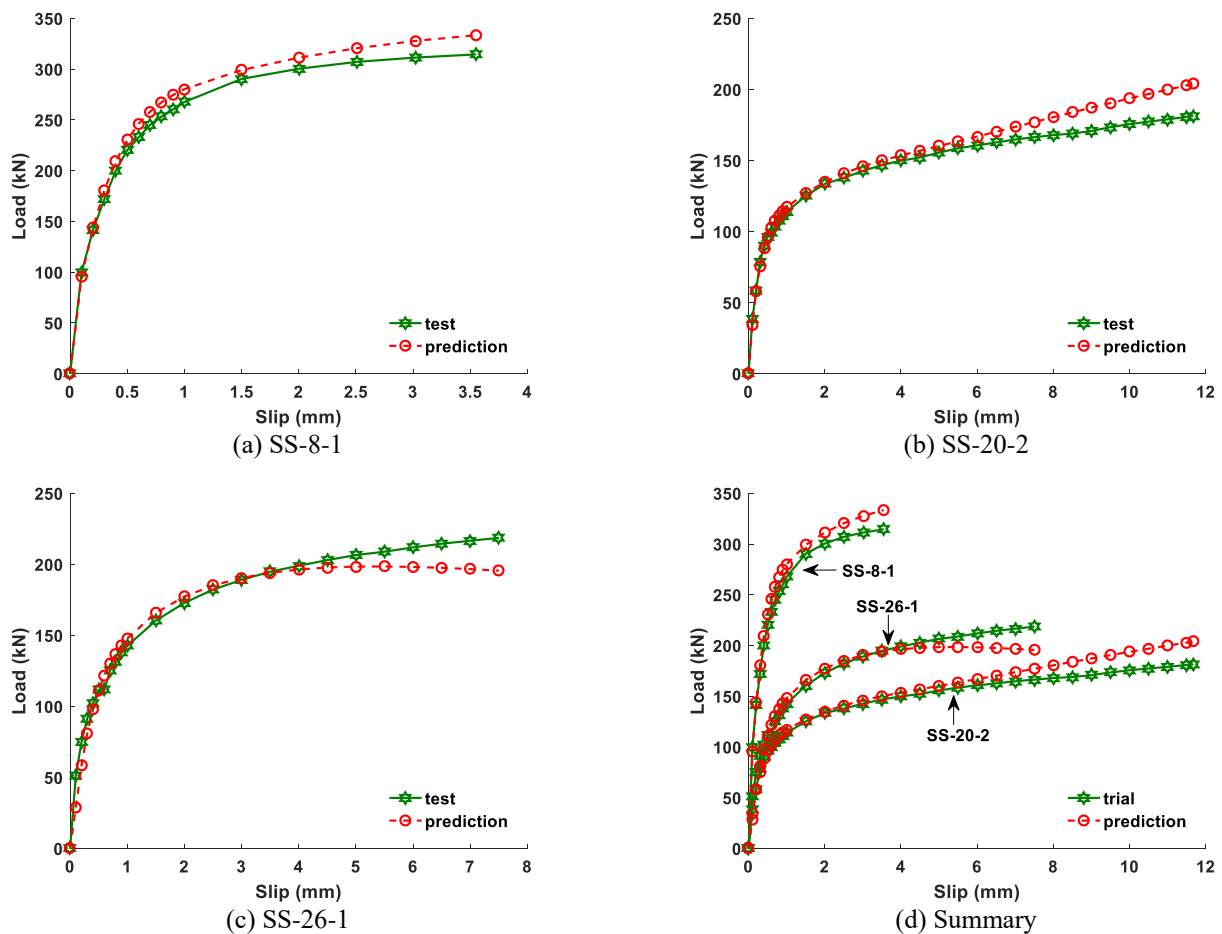


Fig. 6 Comparisons of tests and predictions load-slip curves of stud shear connections

gradually to the peak slip, the prediction load begins to deviate from the test load. The prediction load values of specimens SS-8-1 and SS-20-2 are larger than the test load values, and the specimen SS-26-1 is the opposite. Moreover, the prediction load values of the specimen SS-26-1 shows a slight downward trend, while the test load values of other specimens to train the network are on the rise all the time. The reason for this phenomenon might be that the growth trend of the load is slow and obscure with the slip approaching the peak slip, while there are many input parameters of the neural network which lead to the complexity of the law learned by the network. When a parameter (e.g., the shear stiffness) has an unknown change in the training set, the network may produce abnormal results, which are different from the trend of samples (Karakoç *et al.* 2011).

Compared with only predicting the rising branch of the load-slip curve, the prediction values of the ANN for the whole load-slip curve have larger relative errors. Especially, the absolute errors between the prediction values and the test values of the falling branch of the load-slip curve are large. In the test data set used to train ANNs, it may be due to the different qualities of the connectors or the change of loading conditions that some pairs of the connectors with the same parameters have quite different falling branches of

load-slip curves. It makes the data of the falling branch less representative, and explains why the performance of the ANN trained with these data is poor. Therefore, this paper only predicted the rising branch of the load-slip curve. If the ANN predicts the falling branch at the same time, more connectors with the same parameters will be needed to obtain more test curves and improve the representativeness of the falling branch data.

Comparisons between prediction results and test results of three specimens are shown in Table 2. The ratios of prediction load to test load are calculated in the table, and the prediction effect of the BP neural network can be judged by the average value and standard deviation of the ratios. The average of ratios of the specimen SS-8-1 is 1.04 and the standard deviation is 0.025, the average of ratios of the specimen SS-20-2 is 1.04 and the standard deviation is 0.049, the average of ratios of the specimen SS-26-1 is 0.96 and the standard deviation is 0.110. The reason why the standard deviation of ratios of the specimen SS-26-1 is larger than that of the other two is that the first three prediction loads, including the zero value, is on the low side. It can be corrected by the growth trend at the beginning of the curve. The standard deviation for all subsequent ratios is actually not large. The absolute values of the deviation between the average values of ratios of the

Table 2 Comparisons between test results and prediction results of stud shear connections

Slip (mm)	(1) test load (kN)			(2) prediction load (kN)			(2) / (1)		
	SS-8-1	SS-26-1	SS-20-2	SS-8-1	SS-26-1	SS-20-2	SS-8-1	SS-26-1	SS-20-2
0.10	99.7	51.4	38.6	95.7	28.8	34.4	0.96	0.56	0.89
0.20	141.6	75.1	58.6	143.6	58.6	58.2	1.01	0.78	0.99
0.30	172.1	91.6	78.7	180.9	81.0	75.3	1.05	0.88	0.96
0.40	200.1	102.3	90.4	209.2	98.0	88.5	1.05	0.96	0.98
0.50	220.2	111.7	96.4	230.4	111.2	96.3	1.05	1.00	1.00
0.60	232.9	111.8	99.5	246.3	121.6	102.7	1.06	1.09	1.03
0.70	245.2	125.5	103.7	258.2	130.0	107.6	1.05	1.04	1.04
0.80	253.3	131.1	107.8	267.3	137.0	111.4	1.06	1.04	1.03
0.90	260.3	137.8	111.0	274.5	142.8	114.5	1.05	1.04	1.03
1.00	267.7	142.6	113.9	280.3	147.9	117.2	1.05	1.04	1.03
1.50	290.4	160.4	125.1	299.1	165.9	127.2	1.03	1.03	1.02
2.00	300.4	172.9	133.5	311.3	177.3	134.8	1.04	1.03	1.01
2.50	307.2	182.2	137.8	320.7	185.1	141.0	1.04	1.02	1.02
3.00	311.4	189.1	142.7	327.8	190.4	145.9	1.05	1.01	1.02
3.50	314.5	194.8	146.8	333.4	194.0	150.0	1.06	1.00	1.02
4.00		199.0	149.9		196.4	153.6		0.99	1.02
4.50		203.0	152.2		197.8	156.9		0.97	1.03
5.00		206.5	155.6		198.4	160.2		0.96	1.03
5.50		208.9	158.6		198.5	163.5		0.95	1.03
6.00		211.9	160.7		198.2	166.9		0.94	1.04
6.50		214.5	162.7		197.5	170.3		0.92	1.05
7.00		216.6	164.8		196.6	173.7		0.91	1.05
7.50		218.6	166.4		195.6	177.1		0.89	1.06
8.00			167.9			180.5			1.08
8.50			169.0			183.9			1.09
9.00			170.8			187.2			1.10
9.50			173.5			190.5			1.10
10.00			175.6			193.7			1.10
10.50			177.4			196.8			1.11
11.00			179.0			199.9			1.12
11.50			180.8			202.9			1.12

three specimens and 1 are all 4%, and the fluctuation degree of the ratios are within an acceptable range. The overall statistical analysis of ratios of the three specimens shows that the average value is 1.01 and the standard deviation is 0.081. Thus, it is considered that the load-slip curve of the stud shear connection is predicted successfully by the network.

3.2 Perforated shear connection with flange heads

In this section, the data used to train the network and predict the load-slip curve of the perforated shear connection with flange heads are obtained from the

literature (Su *et al.* 2014) with a total of 30 groups. Since the load-slip curve rises slowly or even fluctuates up and down in the later stage, and the peak slips of most specimens are above 15 mm, a large number of data points are selected in the later stage of load-slip curves according to the selection rules of slip values. Those data have adverse effects on the prediction of the overall trend of the curves. In order to avoid the above influence, slip values are only selected from zero to 10 mm according to the rules. When the other conditions except the shear stiffness are the same, the comparisons of 11 pairs in 22 data groups show that the greater the stiffness of the perforated shear connection with flange heads gets, the higher the shear strength becomes.

Table 3 Parameters of test specimens of perforated shear connections with flange heads

Group	$f_{c,m}$ (MPa)	d_{pr} (mm)	t_p (mm)	d_h (mm)	h_p (mm)	N_f (mm)	K (kN/mm)
TPS-1-1	53.1	19.95	16	60	175	4	889.06
TPS-1-2	53.1	19.95	16	60	175	4	897.32
TPS-2-1	53.1	19.95	16	60	150	4	920.21
TPS-2-2	53.1	19.95	16	60	150	4	752.23
TPS-3-1	53.1	19.95	16	60	200	4	844.79
TPS-3-2	53.1	19.95	16	60	200	4	949.28
TPS-4-1	53.1	19.95	12	60	175	4	666.01
TPS-4-2	53.1	19.95	12	60	175	4	642.56
TPS-5-1	53.1	19.95	20	60	175	4	998.24
TPS-5-2	53.1	19.95	20	60	175	4	1049.01
TPS-6-1	53.1	19.95	16	60	175	4	887.39
TPS-6-2	53.1	19.95	16	60	175	4	915.94
TPS-7-1	53.1	19.95	16	60	175	4	913.13
TPS-7-2	53.1	19.95	16	60	175	4	930.14
TPS-8-1	53.1	19.95	16	60	175	3	917.81
TPS-8-2	53.1	19.95	16	60	175	3	896.91
TPS-9-1	53.1	19.95	16	60	175	5	940.55
TPS-9-2	53.1	19.95	16	60	175	5	867.36
TPS-10-1	53.1	19.95	16	50	175	4	899.72
TPS-10-2	53.1	19.95	16	50	175	4	945.23
TPS-11-1	53.1	19.95	16	75	175	4	820.83
TPS-11-2	53.1	19.95	16	75	175	4	827.53
TPS-12-1	53.1	17.28	16	60	175	4	954.92
TPS-12-2	53.1	17.28	16	60	175	4	694.79
TPS-13-1	53.1	15.08	16	60	175	4	828.50
TPS-13-2	53.1	15.08	16	60	175	4	862.80
TPS-14-1	36.9	19.95	16	60	175	4	751.09
TPS-14-2	36.9	19.95	16	60	175	4	625.80
TPS-15-1	59.3	19.95	16	60	175	4	1007.70
TPS-15-2	59.3	19.95	16	60	175	4	1062.62

The conclusion of comparisons of the remaining eight groups is opposite. It may also be because the inaccurate definition of the shear stiffness. Therefore, the shear stiffness is also taken as the input parameter of this section. The key parameters of 30 groups of perforated shear connections with flange heads are summarized in Table 3.

Input parameters of the network used to predict the load-slip curve of the perforated shear connection with flange heads include: the measured value of concrete compressive strength ($f_{c,m}$), the diameter of reinforcing bars (d_{pr}), the plate thickness (t_p), the hole diameter of web (d_h), the connection height (h_p), the flange number (N_f), the shear stiffness (K) and the slip value ($Slip$). The obtained mapping relationship is as follows

$$\text{Mapping} : P = \{f_{c,m}, d_{pr}, t_p, d_h, h_p, N_f, K, Slip\} \rightarrow \text{Load} \quad (4)$$

where $Load$ represents the load on the perforated shear connection with flange heads when the slip value is $Slip$.

27 groups of data are used to train the network and the remaining three data groups are used for the prediction. When it comes to the selection of prediction data sets, three groups of data with large height differences in the later stage of the load-slip curves are selected in order to observe whether the trained BP neural network can accurately predict the curves with large shape differences (Taffese *et al.* 2015).

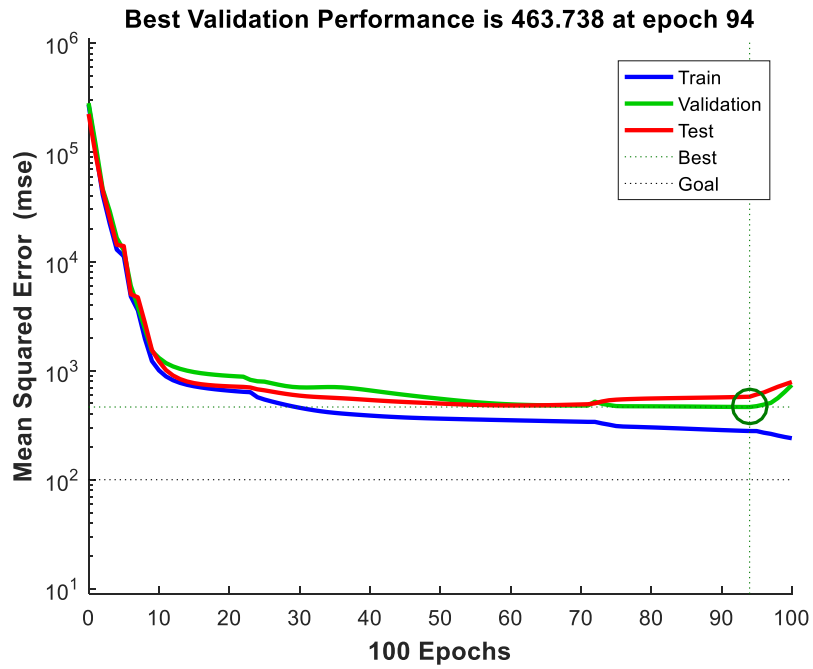


Fig. 7 Error declining curves of perforated shear connections with flange heads

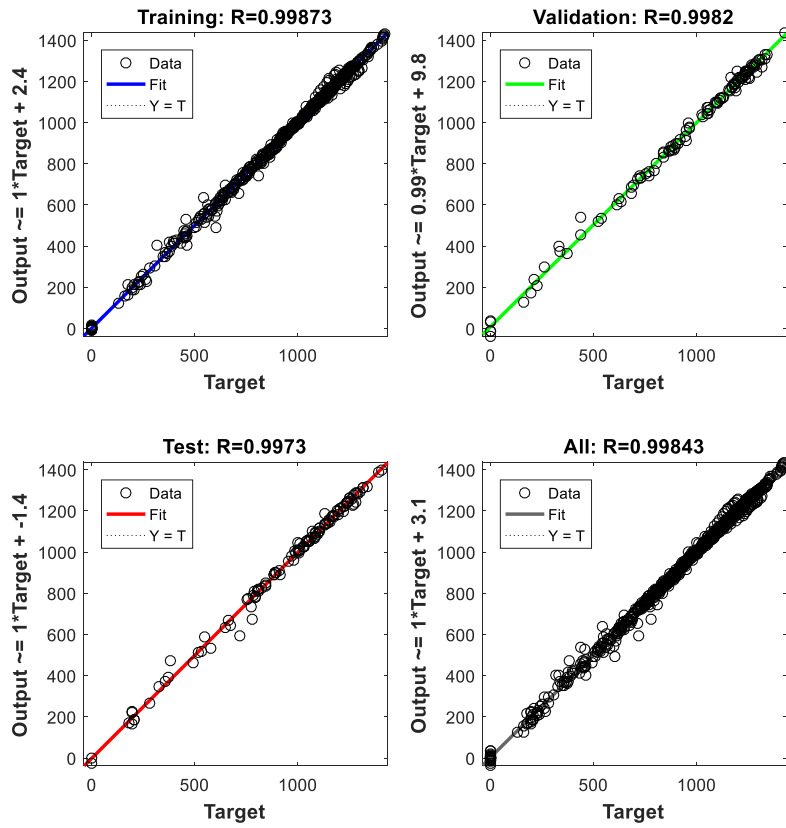


Fig. 8 The degree of correlations between tests and predictions of perforated shear connections with flange heads

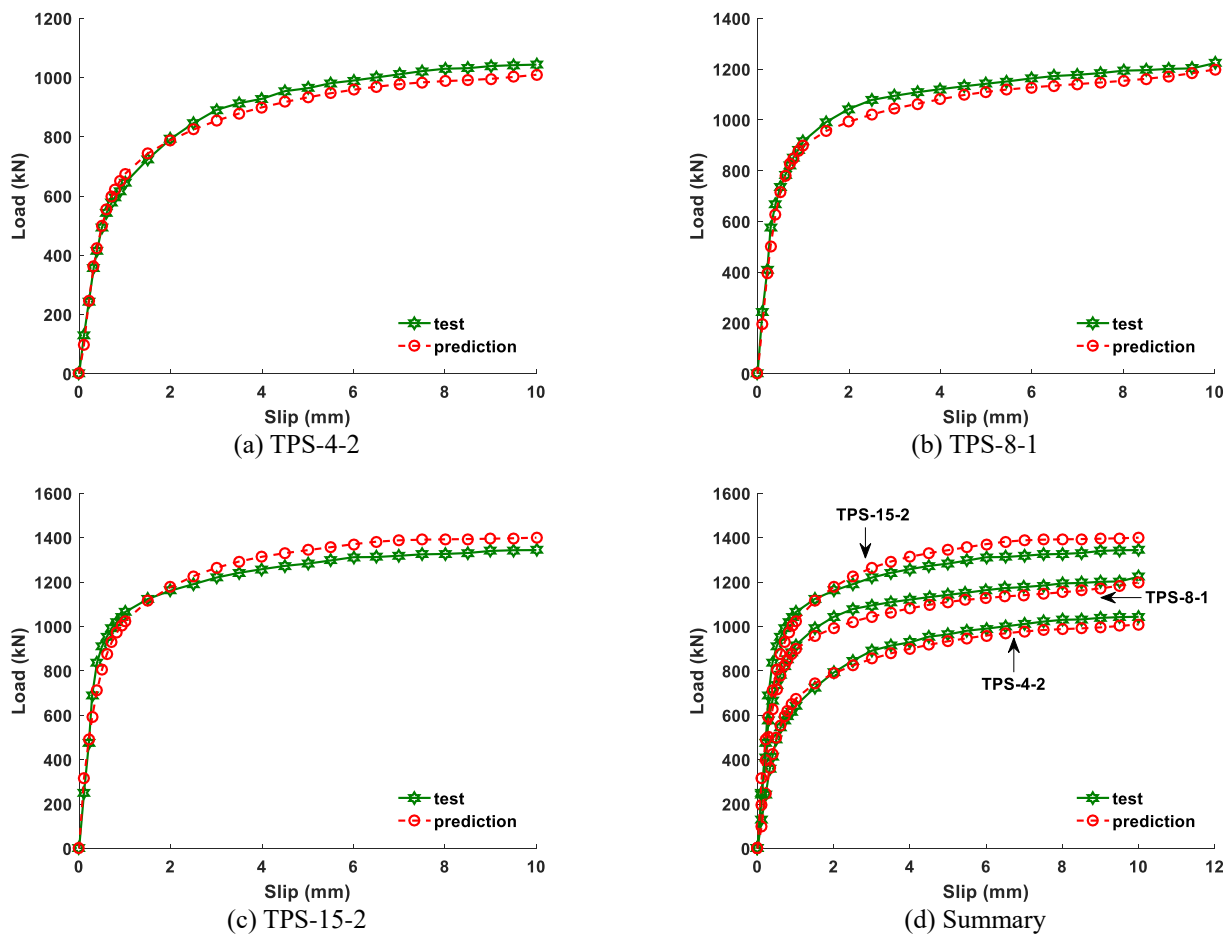


Fig. 9 Comparisons of tests and predictions load-slip curves of perforated shear connections with flange heads

The perforated shear connections with flange heads corresponding to three groups of data used for the prediction are numbered TPS-4-2, TPS-8-1 and TPS-15-2.

When the network is being trained, the target error is set as 100, which is proved impossible to be achieved. When the number of hidden layer nodes increases, the validation error curve of the retrained network doesn't decrease, which indicates the sample data can no longer support the network to learn more profound laws (Chou and Pham 2013). Fig. 7 shows a good training that stops when the network passes 100 iterations and the mean square error is 240, while the validation error curve is the lowest at the 94th iteration. The correlation degree curves of predicted values and experimental values are shown in Fig. 8, and the correlation coefficients between predicted values and experimental values are high. It can be seen from three curves of the training, the test and the validation that each curve has some data points with large deviations. However, the training curve with the most deviation data points has the highest correlation degree, which is due to the dilution of the influence of data with large errors on the correlation between experimental values and predicted values when the number of samples is large (Efstathiades *et al.* 2007). The more data of samples the more bases of the network self-adjustments, and the prediction values would be closer to

the sample data values. Data with large deviations have important influences on the study of stresses and deformations of shear connections. Unless they run counter to the overall trend of the load-slip curve, it is difficult to detect and correct the deviated prediction values.

As is suggested in Fig. 9, the values of the prediction loads are very close to the values of the test loads, which proves that the network can accurately predict the curves with large height differences. The comparisons between prediction results and test results of the three specimens are shown in Table 4. Due to the high shear capacity and the good ductility of the perforated shear connection with flange heads, the failure of the specimen is often marked by the splitting of concrete while the connection is still working. The author failed to collect the data of the falling branch of load-slip curves from the selected literature. The load-slip curves of the connections have the long stable branch after the rising branch. In order to show the accuracy of the ANN prediction of the rising branch better, only the sections with the slip amount of [0, 10 mm] of load-slip curves were taken in Fig. 9. The average value of relative errors of prediction data in table 4 is close to the average value of relative errors of overall prediction data. The average of ratios of the specimen TPS-4-2 is 0.98 and the standard deviation is 0.055, the average of ratios of the

Table 4 Comparisons between test results and prediction results of perforated shear connections with flange heads

Slip (mm)	(1) test load (kN)			(2) prediction load (kN)			(2)/(1)		
	TPS-4-2	TPS-8-1	TPS-15-2	TPS-4-2	TPS-8-1	TPS-15-2	TPS-4-2	TPS-8-1	TPS-15-2
0.10	129.6	243.1	250.1	97.9	196.1	316.8	0.76	0.81	1.27
0.20	242.7	410.6	474.3	246.9	396.2	492.8	1.02	0.96	1.04
0.30	358.2	575.8	689.1	362.8	502.5	591.1	1.01	0.87	0.86
0.40	414.7	667.8	837.8	424.5	626.5	711.7	1.02	0.94	0.85
0.50	492.5	736.3	909.3	498.4	716.1	804.6	1.01	0.97	0.88
0.60	544.3	783.5	953.4	554.7	780.1	875.3	1.02	1.00	0.92
0.70	577.3	821.2	993.5	597.8	826.1	929.3	1.04	1.01	0.94
0.80	596.2	851.9	1019.5	621.1	849.5	971.1	1.04	1.00	0.95
0.90	615.0	882.6	1043.1	649.9	877.0	1004.2	1.06	0.99	0.96
1.00	643.8	915.6	1064.3	674.6	898.0	1023.8	1.05	0.98	0.96
1.50	723.9	991.2	1123.6	743.7	956.3	1114.6	1.03	0.96	0.99
2.00	792.8	1043.1	1161.6	788.6	992.5	1177.5	0.99	0.95	1.01
2.50	846.2	1078.5	1190.7	824.6	1021.3	1226.8	0.97	0.95	1.03
3.00	891.0	1095.0	1220.3	854.4	1044.4	1264.4	0.96	0.95	1.04
3.50	913.8	1109.1	1241.8	878.9	1063.5	1292.8	0.96	0.96	1.04
4.00	928.4	1120.9	1258.1	899.7	1081.3	1314.1	0.97	0.96	1.04
4.50	954.3	1132.7	1273.0	917.7	1098.4	1330.5	0.96	0.97	1.05
5.00	964.3	1142.2	1283.3	933.4	1110.3	1343.9	0.97	0.97	1.05
5.50	981.1	1151.6	1297.1	947.1	1119.6	1357.1	0.97	0.97	1.05
6.00	990.2	1163.4	1312.1	959.1	1128.2	1370.9	0.97	0.97	1.04
6.50	1000.7	1172.9	1312.9	969.2	1134.9	1381.9	0.97	0.97	1.05
7.00	1011.2	1177.6	1318.6	977.6	1141.1	1388.2	0.97	0.97	1.05
7.50	1021.9	1184.4	1324.9	983.9	1147.4	1391.1	0.96	0.97	1.05
8.00	1030.0	1194.1	1326.8	988.2	1154.1	1392.5	0.96	0.97	1.05
8.50	1031.8	1196.2	1331.0	991.4	1161.9	1393.8	0.96	0.97	1.05
9.00	1038.9	1201.2	1340.4	995.9	1171.6	1395.3	0.96	0.98	1.04
9.50	1042.1	1203.0	1343.6	1002.2	1183.8	1397.4	0.96	0.98	1.04
10.00	1043.9	1223.7	1344.1	1009.7	1198.9	1400.1	0.97	0.98	1.04

specimen TPS-8-1 is 0.96 and the standard deviation is 0.039, the average of ratios of the specimen TPS-15-2 is 1.01 and the standard deviation is 0.080. The deviation between the average value of ratios of the three specimens and 1 is less than 4%, and the standard deviation of ratios is all below 0.1. The average value of ratios of the three specimens is 0.99 and the standard deviation is 0.063. Therefore, it can be concluded that the BP neural network is successful in predicting the load-slip curve of the perforated shear connection with flange heads.

4. Conclusions

The following conclusions can be drawn from the model and the analysis in this paper.

(1) A load-slip curve prediction method of shear connections based on ANNs is obtained. The load-slip curves of two different forms of shear connections, the stud shear connection and the perforated shear connection with flange heads, are predicted by using the networks. The results show that the load-slip prediction curves are close to the test results, and the neural networks are successful in predicting two different forms of shear connections.

(2) Due to the deficiency of sample data, the network model does not completely get the influence mechanism of various influencing factors on the load change of shear connections. The network is not very sensitive to changes of key parameters. There is a dependence on the shear stiffness control groups during the trend prediction, thus more the shear stiffness control groups are needed to weaken this influence.

(3) When the load-slip curve is taken as the prediction target of the ANN, there is no special attention paid to the special points on the curve, such as the corresponding point of the peak slip, in which case the prediction of the BP neural network is not as accurate as the traditional formula of the constitutive relation. This problem can be solved by establishing neural networks responsible for predicting the peak slip and the shear strength of shear connections.

Acknowledgments

This research is sponsored by National Natural Science Foundation of China (No. 51808308 and No. 51978351) and State Key Laboratory of Disaster Reduction in Civil Engineering, Tongji University, China (No. SLDRCE17-02). This support is gratefully acknowledged.

References

- Ahn, J.H., Kim, S.H. and Jeong, Y.J. (2008), "Shear behaviour of perfobond rib shear connection under static and cyclic loadings", *Mag. Concrete Res.*, **60**(5), 347-357. <https://doi.org/10.1680/mac.2007.00046>.
- Al-Shamiri, A.K., Kim, J.H., Yuan, T.F. and Yoon, Y.S. (2019), "Modeling the compressive strength of high-strength concrete: An extreme learning approach", *Constr. Build. Mater.*, **208**, 204-219. <https://doi.org/10.1016/j.conbuildmat.2019.02.165>.
- Bonilla, J., Bezerra, L.M. and Mirambell, E. (2019), "Resistance of stud shear connectors in composite beams using profiled steel sheeting", *Eng. Struct.*, **187**, 478-489. <https://doi.org/10.1016/j.engstruct.2019.03.004>.
- Bui, D.K., Nguyen, T., Chou, J.S., Nguyen-Xuan, H. and Ngo, T.D. (2018), "A modified firefly algorithm-artificial neural network expert system for predicting compressive and tensile strength of high-performance concrete", *Constr. Build. Mater.*, **180**, 320-333. <https://doi.org/10.1016/j.conbuildmat.2018.05.201>.
- Chou, J.S. and Pham, A.D. (2013), "Enhanced artificial intelligence for ensemble approach to predicting high performance concrete compressive strength", *Constr. Build. Mater.*, **49**, 554-563. <https://doi.org/10.1016/j.conbuildmat.2013.08.078>.
- Chu, T.H.V., Bui, D.V., Le, V.P.N., Kim, I.T., Ahn, J.H. and Dao, D.K. (2016), "Shear resistance behaviors of a newly puzzle shape of crestbond rib shear connector: An experimental study", *Steel Compos. Struct.*, **21**(5), 1157-1182. <https://doi.org/10.12989/scs.2016.21.5.1157>.
- Ding, F.X., Yin, G.A., Wang, H.B., Wang, L.P. and Guo, Q. (2017), "Behavior of headed shear stud connectors subjected to cyclic loading", *Steel Compos. Struct.*, **25**(6), 705-716. <https://doi.org/10.12989/scs.2017.25.6.705>.
- Efstathiades, C., Baniotopoulos, C.C., Nazarko, P., Ziemianski, L. and Stavroulakis, G.E. (2007), "Application of neural networks for the structural health monitoring in curtain-wall systems", *Eng. Struct.*, **29**(12), 3475-3484. <https://doi.org/10.1016/j.engstruct.2007.08.017>.
- Gu, J.C., Liu, D., Deng, W.Q. and Zhang, J.D. (2019), "Experimental study on the shear resistance of a comb-type perfobond rib shear connector", *J. Constr. Steel Res.*, **158**, 279-289. <https://doi.org/10.1016/j.jcsr.2019.03.032>.
- Hallmark, R., Collin, P. and Hicks, S.J. (2019), "Post-installed shear connectors: Fatigue push-out tests of coiled spring pins", *J. Constr. Steel Res.*, **153**, 298-309. <https://doi.org/10.1016/j.jcsr.2018.10.017>.
- Hammoudi, A., Moussaceb, K., Belebchouche, C. and Dahmoune, F. (2019), "Comparison of artificial neural network (ANN) and response surface methodology (RSM) prediction in compressive strength of recycled concrete aggregates", *Constr. Build. Mater.*, **209**, 425-436. <https://doi.org/10.1016/j.conbuildmat.2019.03.119>.
- Hawkins, N.M. (1973), "The Strength of Stud Shear Connectors", *Civil Engineering Transactions*, **CE15** 46-52.
- He, S.H., Fang, Z., Fang, Y.W., Liu, M., Liu, L.Y. and Mosallam, A.S. (2016), "Experimental study on perfobond strip connector in steel-concrete joints of hybrid bridges", *J. Constr. Steel Res.*, **118**, 169-179. <https://doi.org/10.1016/j.jcsr.2015.11.009>.
- He, Y.L., Wu, X.D., Xiang, Y.Q., Wang, Y.H., Liu, L.S. and He, Z.H. (2017), "Mechanical behavior of stud shear connectors embedded in HFRC", *Steel Compos. Struct.*, **24**(2), 177-189. <https://doi.org/10.12989/scs.2017.24.2.177>.
- Hicks and Smith (2014), "Stud shear connectors in composite beams that support slabs with profiled steel sheeting", *Struct. Eng. Int.*, **24**(2). <https://doi.org/10.2749/101686614X13830790993122>.
- Johnson, R. and May, I. (1975), "Partial-interaction design of composite beams", *The Structural Engineer*, **53**(8), 305-311.
- Karakoç, M.B., Demirboğa, R., Türkmen, İ. and Can, İ. (2011), "Modeling with ANN and effect of pumice aggregate and air entrainment on the freeze-thaw durabilities of HSC", *Constr. Build. Mater.*, **25**(11), 4241-4249. <https://doi.org/10.1016/j.conbuildmat.2011.04.068>.
- Kim, K.S., Han, O., Gombosuren, M. and Kim, S.H. (2019), "Numerical simulation of Y-type perfobond rib shear connectors using finite element analysis", *Steel Compos. Struct.*, **31**(1), 53-67. <https://doi.org/10.12989/scs.2019.31.1.053>.
- Lefik, M. (2013), "Some aspects of application of artificial neural network for numerical modeling in civil engineering", *Bulletin of the Polish Academy of Sciences: Technical Sciences*, **61**(1), 39-50. <https://doi.org/10.2478/bpasts-2013-0003>.
- Liu, Y.Q., Zeng, M.G. and Chen, A.R. (2003), "Application and research of shear connection in bridge structures", *J. Harbin Inst. Technol.*, **35**(1), 271-275.
- Lloyd, R.M. and Wright, H.D. (1990), "Shear connection between composite slabs and steel beams", *J. Constr. Steel Res.*, **15**(4), 255-285. [https://doi.org/10.1016/0143-974x\(90\)90050-Q](https://doi.org/10.1016/0143-974x(90)90050-Q).
- Mashhadban, H., Kutanaei, S.S. and Sayarinejad, M.A. (2016), "Prediction and modeling of mechanical properties in fiber reinforced self-compacting concrete using particle swarm optimization algorithm and artificial neural network", *Constr. Build. Mater.*, **119**, 277-287. <https://doi.org/10.1016/j.conbuildmat.2016.05.034>.
- Nasrollahi, S., Maleki, S., Shariati, M., Marto, A. and Khorami, M. (2018), "Investigation of pipe shear connectors using push out test", *Steel Compos. Struct.*, **27**(5), 537-543. [https://doi.org/10.1016/S0092-8240\(05\)80006-0](https://doi.org/10.1016/S0092-8240(05)80006-0).
- Nguyen, G.B. and Machacek, J. (2016), "Effect of local small diameter stud connectors on behavior of partially encased composite beams", *Steel Compos. Struct.*, **20**(2), 251-266. <https://doi.org/10.12989/scs.2016.20.2.251>.
- Nie, J., Cai, C.S. and Wang, T. (2005), "Stiffness and capacity of steel-concrete composite beams with profiled sheeting", *Eng. Struct.*, **27**(7).

- Ning, C.-L., Wang, L. and Du, W. (2019), "A practical approach to predict the hysteresis loop of reinforced concrete columns failing in different modes", *Constr. Build. Mater.*, **218**, 644-656. <https://doi.org/10.1016/j.conbuildmat.2019.05.147>.
- Oehlers, D. and Johnson, R. (1987), "The strength of stud shear connections in composite beams", *The Structural Engineer.*, **65B**(2), 44-48.
- Oguejiofor, E. and Hosain, M. (1994), "A parametric study of perfobond rib shear connection", *Can. J. Civil Eng.*, **21**(4), 614-625. <https://doi.org/10.1139/194-063>.
- Pavlovic, M., Markovic, Z., Veljkovic, M. and Budevaca, D. (2013), "Bolted shear connectors vs. headed studs behaviour in push-out tests", *J. Constr. Steel Res.*, **88**, 134-149. <https://doi.org/10.1016/j.jcsr.2013.05.003>.
- Rosenblatt, F. (1958), "The perception: A probabilistic model for information storage and organization in the brain", *Psychological Review*, **65**, 386-408. <https://doi.org/10.1037/h0042519>.
- Segal, M.M. (1988), "Explorations In Parallel Distributed-Processing - a Handbook Of Models, Programs, And Exercises - McClellan, JI, Rumelhart, De", *Science*, **241**(4869), 1107-1108. <https://doi.org/10.1126/science.241.4869.1107>.
- Shahabi, S.E.M., Sulong, N.H.R., Shariati, M. and Shah, S.N.R. (2016), "Performance of shear connectors at elevated temperatures-A review", *Steel Compos. Struct.*, **20**(1), 185-203. <https://doi.org/10.12989/scs.2016.20.1.185>.
- Su, Q.T., Wang, W., Luan, H.W. and Yang, G.T. (2014), "Experimental research on bearing mechanism of perfobond rib shear connectors", *J. Constr. Steel Res.*, **95**, 22-31. <https://doi.org/10.1016/j.jcsr.2013.11.020>.
- Su, Q.T., Yang, G.T. and Li, C.X. (2014), "Structural behaviour of perforated shear connectors with flange heads in composite girders: an experimental approach", *Int. J. Steel Struct.*, **14**(1), 151-164. <https://doi.org/10.1007/s13296-014-1013-5>.
- Suwaed, A.S.H. and Karavasilis, T.L. (2018), "Removable shear connector for steel-concrete composite bridges", *Steel Compos. Struct.*, **29**(1), 107-123. <https://doi.org/10.12989/scs.2018.29.1.107>.
- Taffese, W.Z., Sistonen, E. and Puttonen, J. (2015), "CaPrM: Carbonation prediction model for reinforced concrete using machine learning methods", *Constr. Build. Mater.*, **100**, 70-82. <https://doi.org/10.1016/j.conbuildmat.2015.09.058>.
- Vianna, J.D., Costa-Neves, L.F., Vellasco, P.C.G.D. and de Andrade, S.A.L. (2008), "Structural behaviour of T-Perfobond shear connectors in composite girders: An experimental approach", *Eng. Struct.*, **30**(9), 2381-2391. <https://doi.org/10.1016/j.engstruct.2008.01.015>.
- Wang, B., Man, T. and Jin, H. (2015), "Prediction of expansion behavior of self-stressing concrete by artificial neural networks and fuzzy inference systems", *Constr. Build. Mater.*, **84**, 184-191. <https://doi.org/10.1016/j.conbuildmat.2015.03.059>.
- Wang, Q. (2013), "Experimental Research on Mechanical Behavior and Design Method of Stud Connectors", *Doctor's dissertation: Tongji University*.
- Wang, Y.C. (1998), "Deflection of steel-concrete composite beams with partial shear interaction", *J. Struct. Eng.*, **124**(10), 1159-1165. [https://doi.org/10.1061/\(ASCE\)0733-9445\(1998\)124:10\(1159\)](https://doi.org/10.1061/(ASCE)0733-9445(1998)124:10(1159)).
- Wei, X., Shariati, M., Zandi, Y., Pei, S.L., Jin, Z.B., Gharachurlu, S., Abdullahi, M.M., Tahir, M.M. and Khorami, M. (2018), "Distribution of shear force in perforated shear connectors", *Steel Compos. Struct.*, **27**(3), 389-399. <https://doi.org/10.12989/scs.2018.27.3.389>.
- Zhao, Z. and Ren, L. (2002), "Failure criterion of concrete under triaxial stresses using neural networks", *Comput.-Aided Civil Infrastruct. Eng.*, **17**, 68-73.
- Zheng, S.J. and Liu, Y.Q. (2014), "Experiment of initial shear stiffness of perfobond connector", *China J. Highway Transport*. **27**(11), 69-75.

BU